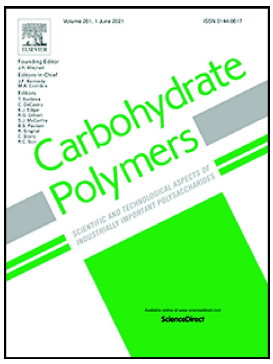

Evolution of the free volume during water desorption in thermoplastic starch/citric acid films: In situ positron annihilation studies

Santiago Estevez-Areco, Carlos Macchi, Lucas Guz, Silvia Goyanes, Alberto Somoza

PII: S0144-8617(23)00203-5

DOI: https://doi.org/10.1016/j.carbpol.2023.120739

Reference: CARP 120739

To appear in: *Carbohydrate Polymers*

Received date: 11 November 2022

Revised date: 7 February 2023

Accepted date: 20 February 2023

Please cite this article as: S. Estevez-Areco, C. Macchi, L. Guz, et al., Evolution of the free volume during water desorption in thermoplastic starch/citric acid films: In situ positron annihilation studies, *Carbohydrate Polymers* (2023), https://doi.org/10.1016/j.carbpol.2023.120739

Evolution of the free volume during water desorption in thermoplastic starch/citric acid films: *in situ* positron annihilation studies

Santiago Estevez-Areco[a,b,*], Carlos Macchi[a,b], Lucas Guz[c], Silvia Goyanes[d,e], Alberto Somoza[a,b]

[a] Universidad Nacional del Centro de la Provincia de Buenos Aires (UNCPBA), Facultad de Ciencias Exactas,, Instituto de Física de Materiales Tandil (IFIMAT), Grupo Positrones "Prof. Alfredo Dupasquier", Pinto 399, (7000) Tandil, Buenos Aires, Argentina

[b] CIFICEN, UNCPBA-CICPBA-CONICET, Tandil, Buenos Aires, Argentina

[c] Instituto de Investigación e Ingeniería Ambiental (IIIA), CONICET, Universidad Nacional de San Martín, (3iA). Campus Miguelete, 25 de mayo y Francia (1650), San Martín, Buenos Aires, Argentina.

[d] Universidad de Buenos Aires. Facultad de Ciencias Exactas y Naturales, Departamento de Física, Laboratorio de Polímeros y Materiales Compuestos (LP&MC). Ciudad Universitaria (C1428EGA), Ciudad Autónoma de Buenos Aires, Argentina.

[e] CONICET - Universidad de Buenos Aires. Instituto de Física de Buenos Aires (IFIBA). Ciudad Universitaria (C1428EGA), Ciudad Autónoma de Buenos Aires, Argentina.

*Corresponding author

E-mail addresses: sestevez@ifimat.exa.unicen.edu.ar (S. Estevez-Areco); cmacchi@ifimat.exa.unicen.edu.ar (C. Macchi); lguz@unsam.edu.ar (L. Guz); goyanes@df.uba.ar (S. Goyanes); asomoza@exa.unicen.edu.ar (A. Somoza).

Abstract

The effect of citric acid (CA) concentration and water content on the free hole volume of thermoplastic cassava starch films (TPS) was studied. To this aim, continuous *in situ* positron annihilation lifetime spectroscopy measurements were performed at fixed moisture content and during water desorption. The results show that the increase in CA concentration leads to wider free hole volume distributions with lower mean values. During water desorption, the mean values and width of such distributions systematically decrease with the exposure time, and the evolution of the hole volumes was well-described using the Kohlrausch-Williams-Watts function. The water vapour permeability was significantly higher in films incorporating 5% (w/w) of CA, in line with the more open network of this material that was revealed in the hole volumes distribution. The Young's modulus of all the developed films increased significantly after partial water desorption, which was attributed to the plasticizer loss reflected in a decrease in the mean hole volume value (between 4% and 13%). This work evidences that the control and report of the relative humidity are essential when testing TPS-based films, as their nanostructures are strongly dependent on external conditions.

Keywords: Thermoplastic starch; Citric acid; Free hole volume; Positron annihilation lifetime spectroscopy.

1. Introduction

Petroleum-based plastics manufacturing has dramatically increased in the last decades, reaching a global production of more than 380 million tons annually (Geyer, 2020). The extensive use of plastic products has led to a huge garbage dump, which mostly ends in the environment because of the lack of proper policies or inefficient waste management systems. Biobased and biodegradable plastics

constitute an alternative to conventional ones that could contribute to mitigating the environmental impact. From this point of view, the development of this kind of plastics has many advantages, such as diverting from fossil resources, introducing new recycling or degradation pathways, and using less toxic reagents and solvents in production processes (Rosenboom et al., 2022).

Starch has been proposed as a raw material for the production of bioplastics because it is renewable, widely available, low-cost, biodegradable, and compostable (Wang et al., 2020). Starch granules are isolated from many sources (wheat, rice, potato, cassava, among others), and they can be processed by scalable technologies –extrusion, moulding, blow moulding- to obtain thermoplastic starches (TPS) as pellets or films, by the addition of plasticizers to overcome the brittleness and facilitate the processability (Guz et al., 2020; Zhang et al., 2014).

Pure TPS materials present a pronounced hydrophilicity and hygroscopic character, which leads to poor moisture barrier, high solubility, and a dependence of the mechanical properties on the ambient humidity (Medina Jaramillo et al., 2015; Ribba et al., 2017). To overcome these issues, several approaches have been proposed, including the incorporation of micro- and nanoparticles, adding low molecular weight components -such as natural extracts-, and chemical or physicochemical modifications (Diyana et al., 2021; Estevez-Areco et al., 2019; Florez et al., 2019; Guarás et al., 2020; Guz et al., 2020). The addition of citric acid (CA) to TPS matrices has been widely studied because it can improve materials stability and diminish water susceptibility (Gonzalez-Seligra et al., 2016; Reddy & Yang, 2010; Shi et al., 2007). The main mechanisms responsible for the mentioned stabilization are esterification and crosslinking. Additionally, CA is considered an interesting green crosslinker for carbohydrate polymeric materials (Salihu et al., 2021).

Free volume theory allows explaining different properties of polymeric systems, such as glass transition, viscosity, molecular transport, and permeability (Giacinti Baschetti & De Angelis, 2015; Langer et al., 2020; Shakespeare, 2002). Free volume can be quantitatively described by the size, distribution, and total amount of sub-nanometer holes. Positron annihilation lifetime spectroscopy (PALS) is the only experimental technique capable of determining the free hole volume (v_h) and free volume fractions (f_v) in polymeric materials (Dlubek et al., 2000; Jean, 1990; Jean et al., 2003).

Several researchers have used PALS to study carbohydrate polymer materials. In particular, Hughes et al. (2016) and Martini et al. (2020) have reported that water activity in modified starch-sucrose blends influences the free volume properties. It was reported that water susceptibility affects the free volume because the water uptake rate is directly related to the moisture content of the samples. PALS studies about water susceptibility in glassy carbohydrates were also reported by Kilburn et al. (2004, 2005). Recently, the differences in the sorption capacity of cellulose films with different esterification degrees were correlated with the filling of excess free volume (Chalykh et al., 2021). On the other hand, Roussenova et al. (2010) carried out a systematic study on plasticization, antiplasticization, and molecular packing in amorphous carbohydrate-glycerol matrices. However, only a few works were focused on the study of TPS films (Cheng et al., 2021; Lin et al., 2010). It deserves to be mentioned that Lin et al. (2010) reported that the free hole volume increased after a soak steam treatment in TPS-cellulose films, but no significant differences in the hole volumes were found when similar films with a hydrophobic coating were subjected to the same treatment.

The novelty of the present work is the study of the evolution of the free hole volume in time as a consequence of the hygroscopic character of the TPS-based films. To the best of our knowledge, there are no systematic studies regarding this issue. Neither have we found reported results on PALS studies regarding the effect of CA, or other organic acids, on the free volume of polysaccharides. In the present work, we hypothesized that free hole volumes of thermoplastic starch films depend on

the citric acid concentration and vary during water desorption. To address this investigation, continuous PALS measurements of TPS-based films with different CA concentrations were carried out. Firstly, the structure of the different TPS-CA films was determined at fixed equilibrium humidity. Secondly, samples of each material were placed into a drier atmosphere and the hole sizes were measured during water desorption.

2. Materials and Methods

2.1 Fabrication of thermoplastic starch films

2.1.1 Materials

Cassava Starch (18% amylose $\sim 1.5 \times 10^5$ g/mol; 82% amylopectin $\sim 10^8$ g/mol) was supplied by Cooperativa Agrícola e Industrial San Alberto Limitada (C.A.I.S.A., Misiones, Argentina). Analytical grade glycerol (Sigma-Aldrich, Germany), industrial grade sorbitol (Mapal, Argentina), anhydrous citric acid (Stanton, Argentina), and sodium hypophosphite 1-hydrate p.a. (Biopack, Argentina) were used as received.

2.1.2 Thermoplastic starch films fabrication

TPS-based films were fabricated in a single step using flat-die extrusion followed by calendaring. Water, glycerol, and sorbitol were used as plasticizers at a fixed ratio (20% w/w of water to starch; 15% w/w of glycerol/sorbitol to starch) following a recent article (Estevez-Areco et al., 2020). Different amounts of CA were incorporated into the powdered mixtures before extrusion to obtain different TPS-CA films (0, 1, and 5% w/w to starch). Sodium hypophosphite was used as a catalyst for esterification reactions and it was incorporated at a fixed ratio of CA (1:2 w/w) (Reddy & Yang, 2010). Table 1 presents the compositions of the different systems.

Table 1. Nomenclature and composition of the different mixtures.

Nomenclature	Starch (%)	Water (%)	Glycerol (%)	Sorbitol (%)	CA (%)	Sodium hypophosphite (%)
TPS	66.6	13.4	10.0	10.0	0.0	0.0
TPS-CA1	66.0	13.2	9.9	9.9	0.66	0.33
TPS-CA5	63.5	12.7	9.5	9.5	3.18	1.59

Firstly, citric acid and sodium hypophosphite were dissolved in a water, glycerol, and sorbitol solution using a magnetic stirrer (90°C, 20 min). Then, solutions were incorporated into cassava starch and manually mixed until complete absorption of the liquid phase. The obtained powdered mixtures were homogenized in a homemade horizontal triple ribbon mixer (20 rpm, 15 min), sieved with a mesh (2 mm), and stored for 24 h in sealed containers before extrusion.

Extrusion was carried out using a co-rotating twin screw extruder (Nanjing Kerke Extrusion equipment Co., Ltd., Jiangsu, China) with a screw diameter of 16 mm, a length of 640 mm and a flat die of 32 mm x 1.5 mm. The extruder features ten independent heating zones and has a ventilation valve in the eighth zone. Screw speed (80 rpm) and temperature profile (90-100-110-120-120-130-130-140-130-120°C, from the feeder to the die) were selected to obtain a complete thermo-plasticized material (González-Seligra et al., 2017). A calender at 120°C was coupled to the flat die to homogenize and reduce film thickness. The obtained materials were stored at room temperature (20°C) in a desiccator containing an oversaturated sodium bromide (NaBr) solution, resulting in relative humidity (RH) of 58%, at least 4 weeks before the test (Famá et al., 2007).

2.2 Physicochemical characterizations

Thermogravimetric analysis (TGA), Fourier-transform infrared spectroscopy (FTIR) and scanning elec-

tron microscopy were performed to characterize the samples. Methodology, results, and discussion of these characterizations are included in Supplementary Material.

2.2.1 PALS system set-up

Positron annihilation lifetime spectroscopy measurements were carried out in air at room temperature (RT) using a fast-fast coincidence spectrometer with a lifetime resolution (FWHM) of 340 ps. A 20 µCi positron source was prepared by depositing an aqueous ^{22}NaCl solution onto a thin Kapton foil (7.5 µm thick). The source was sandwiched between two identical samples (thickness~0.5 mm, mass~20 mg).

Materials at fixed moisture content were studied by placing the stabilized samples (RH=58%) together with the source in polypropylene-sealed bags before PALS measurements. This experimental arrangement allows the samples to retain their humidity content during measurements, avoiding exchange with the laboratory atmosphere.

For structural determinations during water desorption, the stabilized samples (RH=58%) together with the positron source, were placed into polypropylene-sealed bags containing ~10 g of silica gel. The silica gel had previously been dried overnight at 105 °C, producing an atmosphere with RH of 20%. PALS spectra were continuously measured for about 6 consecutive days without dismounting the sample from the spectrometer and during water desorption of the material. Considering that the mass of the samples is negligible compared to the mass of silica gel and because there is no exchange between the sealed bag and the outside environment, the relative humidity remained constant during measurements.

In both cases, PALS spectra containing at least 1.5×10^6 counts were collected for each sample in the above-mentioned conditions, and the PALS parameters reported in this work were obtained as an average of 5 measurements.

2.2.2 PALS model

According to the common interpretation for PALS spectra in polymers (Jean, 1990), the shortest lifetime component τ_1 (0.15 – 0.3 ns) is ascribed to positrons annihilated into the bulk and to para-Positronium (p-Ps) annihilations, and the intermediate lifetime component τ_2 (0.35-0.60 ns) is attributed to positrons annihilated in low electron density regions of the samples. The long-lived lifetime component τ_3 (1.5-2.2 ns) is attributed to the ortho-Positronium (o-Ps) annihilation process (via pick-off) trapped in the nanoholes forming the free volume ($\tau_3 \equiv \tau_{o\text{-}Ps}$). The values of $\tau_{o\text{-}Ps}$ can be correlated with the average radius of the free volume holes (r_h) probed by the o-Ps, assuming a spherical approximation and using the semi-empirical Tao-Eldrup model (Eq. 1) (Eldrup et al., 1981):

$$\lambda_{o-Ps} = \frac{1}{\tau_{o-Ps}(r_h)} = 0.5\left[\frac{\delta r_h}{r_h+\delta r} + \frac{1}{2\pi} sin\left(\frac{2\pi r_h}{r_h+\delta r}\right)\right] \quad , \quad (1)$$

where δr=0.166 nm is an empirical parameter that describes the penetration of the Ps wave function into the molecular electron layer surrounding the free volume hole in which the o-Ps is localized.

Positron annihilation contributions from each of the three above-mentioned states were obtained using the LT10 program (Giebel & Kansy, 2011), where the shape of the o-Ps annihilation rate distribution, $\alpha_3(\lambda_{o-Ps})$, is assumed to take a log-normal distribution. The mean value ($\tau_{o\text{-}Ps}$), its dispersion ($\sigma_{o\text{-}Ps}$) and the relative intensity ($I_{o\text{-}Ps}$) associated with the o-Ps lifetime distributions were obtained from the analysis. The $\sigma_{o\text{-}Ps}$ values can be interpreted as the heterogeneity levels in the local free hole volume. Larger $\sigma_{o\text{-}Ps}$ values indicate broader free hole volume distributions.

Following the model proposed by Dlubek et al. (2004) to analyze PALS spectra assuming a dispersion in the o-Ps lifetime component, using the obtained $\alpha_3(\lambda_{o-Ps})$ distributions and the Eq. 1, the hole

radius probability distribution $n(r_h)$ can be calculated as:

$$n(r_h) = -\alpha_3(\lambda_{o-Ps})\frac{d\lambda_{o-Ps}}{dr_h} = -3.32\left\{cos\left(\frac{2\pi r_h}{r_h+\delta R}\right)-1\right\}\frac{\alpha_3(\lambda_{o-Ps})}{(r_h+\delta R)^2} \quad (2)$$

Using the $n(r_h)$ distributions presented in Eq. 2, the volume fraction hole size $g(v_h)$ and the number fraction hole $g_n(v_h)$ distributions can be derived as follows:

$$g(v_h) = \frac{n(r_h)}{4\pi {r_h}^2} \quad (3)$$

$$g_n(v_h) = \frac{g(v_h)}{v_h} \quad (4)$$

Using Eq. 1, the v_h obtained are discrete free hole volume values; under the frame of mathematical statistics, the mean value of the number-weighted hole volume distribution and its dispersion can be calculated according to:

$$\langle v_h \rangle = \int v_h g_n(v_h)\, dv_h \quad (5)$$

$$\sigma_h = \sqrt{\int (v_h - \langle v_h \rangle)^2 g_n(v_h)\, dv_h} \quad (6)$$

where the $g_n(v_h)$ distribution is normalized to the unity area below the curve.

The simplest approach to calculating the fractional free volume from the positron data assumes that the number of nanoholes forming the free volume is represented by I_{o-Ps} (Kobayashi et al., 1989). The presence of carboxylic acid groups in TPS-CA films could partially inhibit the positronium formation by scavenging electrons: hence, in this research the I_{o-Ps} parameter was not considered.

2.2.2 Water susceptibility

Moisture content (MC) was determined according to the standard method of the AOAC (Cunniff & Jee, 1995). Samples of each system (m_w~0.5 g) were dried in an oven at 105°C for 24 h and then weighed (m_d). Moisture content was then calculated using Eq. 7:

$$MC(\%) = 100\frac{m_w - m_d}{m_w}. \quad (7)$$

Water solubility (WS) was determined following the procedure described by Maizura, Fazilah, Norziah, & Karim (2007), with some modifications. Samples of films (1.6 cm diameter discs) were weighed and the moisture content was subtracted to obtain the initial dried mass (m_{si}). The samples were submerged in deionized water (50 mL, 20°C, 24 h) under constant agitation. Film remnants were separated by filtration, and dried at 105°C to constant mass (m_{sf}). WS was calculated using Eq. 8:

$$WS(\%) = 100\frac{m_{si} - m_{sf}}{m_{si}}. \quad (8)$$

Water vapour permeability (WVP) of films was measured using a modified ASTM E96-00 procedure (Famá et al., 2012). Samples were placed into circular acrylic cells containing $CaCl_2$, located in desiccators containing an oversaturated sodium chloride (NaCl) solution, resulting in RH of 75%. The cells' weight was measured for 10 consecutive days, and the water vapour transport (WVT) was determined as the slope from the weight curve as a function of time divided by the cell area (3.8 cm^2). WVP was calculated using Eq. 9, where *e* is the film thickness and P_0 is the saturation vapour pressure of water at room temperature.

$$WVP = \frac{WVTe}{P_0 RH}. \quad (9)$$

Parameters describing the susceptibility to water were reported as the average of at least three independent experiments.

2.2.3 Mechanical properties

Uniaxial tensile tests were performed using a Brookfield Texture Analyzer (CT3-100) according to ASTM-D882-02 (ASTM Standard, 2004). Probes of 35 mm x 5 mm (length x width) were tested at a strain rate of 10^{-3} s^{-1}. Thickness was measured for each sample and Young's modulus (E) was calcu-

lated as the slope of the linear fitting of the first 0.5% of deformation. As described above, the probes were previously stabilized in a desiccator at RH=58%. The samples were tested immediately after the desiccator was opened (*t=0*), then exposed to the lab atmosphere (RH=45%), and tested again after 5 h.

2.2.4 Data processing and statistical analysis

Data were analyzed using two-way ANOVA with 95% confidence level ($p < 0.05$) and Tukey post-hoc test.

3. Results and discussion

The analysis of SEM, FTIR, and TGA-DTA is presented in the Supplementary Material. Briefly, SEM images show that starch granules were completely thermo-plasticized after the fabrication of TPS and TPS-CA films and a unique phase was observed; FTIR spectra reveal that increasing CA content leads to a higher esterification degree; TGA-DTA curves show a slight decrease of degradation temperatures of starch for higher CA content.

The main body of this paper was focused on the free volume properties of TPS-CA films and their relationship with water susceptibility and mechanical properties. The analysis of the results was divided into two sub-sections: first, the influence of citric acid concentration on the hole sizes of the films stored at equilibrium conditions (RH=58%) is introduced (Section 3.1); then, the effect of water desorption on the hole sizes of the different materials is presented (Section 3.2).

3.1 Influence of CA on the free hole volume of TPS-based films

Table 2 presents the average ortho-Positronium lifetime values and their associated dispersions obtained from the PALS spectra decompositions. Lifetime values varied slightly between the different thermoplastic starch samples, ranging from 1.65 to 1.67 ns. No significant differences ($p < 0.05$) were observed between the parameters characterizing TPS and TPS-CA films. However, a tendency to higher $\sigma_{o\text{-}Ps}$ values was observed when increasing the citric acid concentration.

Table 2. Mean lifetime values (τ_{o-Ps}) with their associated dispersions ($\sigma_{o\text{-}Ps}$). The values are reported as average ± standard error.

	τ_{o-PS} (ns)	$\sigma_{o\text{-}Ps}$ (ns)
TPS	1.667 ± 0.008[a]	0.22 ± 0.02[a]
TPS-CA1	1.648 ± 0.009[a]	0.24 ± 0.02[a]
TPS-CA5	1.65 ± 0.01[a]	0.28 ± 0.02[a]

Different letters within the same column indicate statistically significant differences ($p < 0.05$).

Figure 1 presents the obtained distributions for the free hole volumes of the different TPS-based films. The mean value of hole volumes as a function of CA concentration is plotted in the inset. The most representative statistical parameters of the right-skewed distributions, which are mean, dispersion, mode, and left/right semi-widths at half height, are reported in Table 3.

The mean hole volume of TPS film was ~70 Å^3. The obtained value is within the range of other carbohydrates, even though there is no reported data on free volumes in thermoplastic starch films. For example, it has been reported hole volumes of 28-30 Å^3 and ~47 Å^3 for glassy and amorphous maltodextrin samples, respectively (Kilburn et al., 2004, 2005), values in the range 42-61 Å^3 for maltodextrin-glycerol matrixes (Roussenova et al., 2010), and a mean hole volume of (37 ± 3) Å^3 for hydrophobically-modified starch (Hughes et al., 2016). As described in the literature, the free hole volumes vary with plasticizers content, so it should be highlighted that the results reported in the present research correspond to thermoplastic starch films plasticized with sorbitol, glycerol, and

water in the ratios described before (Table 1, Section 2.1.2).

The incorporation of CA modified the hole volume distribution. It was observed a tendency to lower values in the obtained $\langle v_h \rangle$ when CA was incorporated in the formulations, although there were no significant differences (Table 3 and inset in Fig. 1). Moreover, the most probable value (mode) decreased with increasing CA content. The decrease in both values can be related to the ester bonding between citric acid and starch chains (Supplementary Material), which reduces chain mobility. On the other hand, the width of the hole volume distribution increases with increasing CA content, and there is a larger number of holes with volumes in the range of 100-140 Å^3 in TPS-CA5. This effect could be related to the higher moisture content of this material, as will be discussed in Section 3.3.

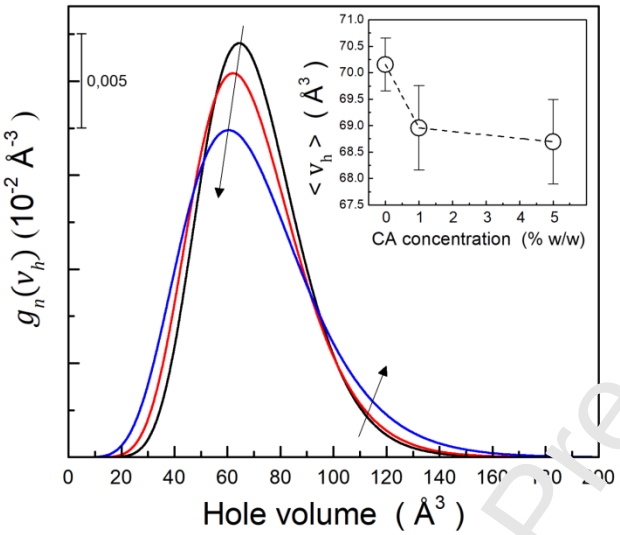

Figure 1. Hole volume probability distributions for the TPS (—), TPS-CA1 (—) and TPS-CA5 (—) films stabilized at RH=58%. The inset shows the mean value of the hole volume to CA concentration. In the inset, dashed lines are only eye guides.

Table 3. Statistical parameters associated with the hole volume distributions for the TPS, TPS-CA1, and TPS-CA5 samples. H_- and H_+ are the left and right semi-widths at half height of the hole volume probability distributions, respectively. The values are reported as average ± standard error.

	$\langle v_h \rangle$ (Å^3)	σ_v (Å^3)	Mode (Å^3)	H_- (Å^3)	H_+ (Å^3)
TPS	70.1 ± 0.5^a	19 ± 2	64.3 ± 1.2^a	18 ± 1^a	24 ± 3^a
TPS-CA1	69 ± 1^a	21 ± 2^a	62.0 ± 1.5^{ab}	19.5 ± 1^a	26 ± 3^a
TPS-CA5	69 ± 1^a	25 ± 2^b	60.5 ± 1.5^b	22 ± 1^b	31 ± 2^b

Different letters within the same column indicate statistically significant differences ($p < 0.05$).

3.2 Influence of the CA content and exposure time during water desorption on the free hole volume

Figure 2 presents the mean hole volume evolution of the different samples during water desorption. In this set of experiments, the initial state corresponds to the stabilized samples characterized in the previous section (stabilized at RH=58%). Water acts as a plasticizer of thermoplastic starch, and the moisture loss leads to lower plasticizer content in the samples. Thus, the obtained results show structural changes as a consequence of the continuous decrease of the plasticizer content. All samples presented a systematic decrease of the mean hole volume with time, which stabilized after 100-120 h. The asymptote represents the free hole volume of the samples at the new equilibrium state, which depends on the proposed relative humidity. It can be observed that the $\langle v_h \rangle$ value corre-

sponding to the equilibrium state at RH=20 has decreased with increasing CA concentration in the films. Besides, the kinetic of the process was slower in the TPS sample to TPS-CA1 and TPS-CA5 samples.

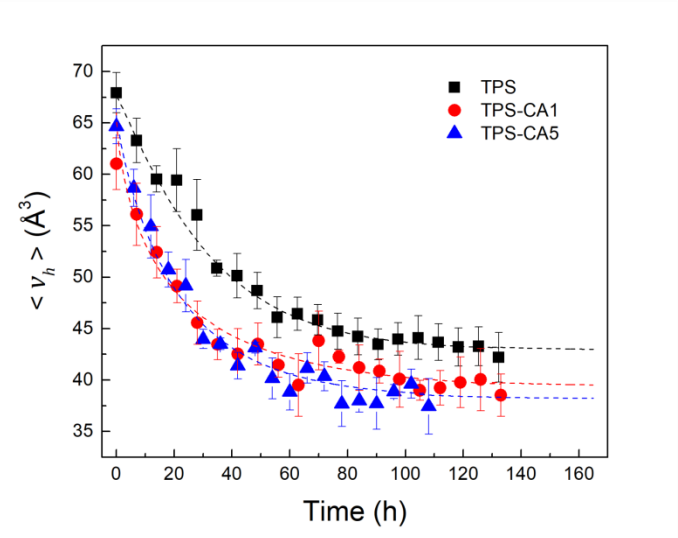

Figure 2. Mean hole volume as a function of the elapsed time at RT and RH=20%. Dashed lines correspond to the best fit of the experimental data using the KWW function.

The experimental results of mean hole volume as a function of time were fitted with the Kohlrausch-Williams-Watts (KWW) function:

$$\frac{v_h(t)-v_h^{\infty}}{v_h^{0}-v_h^{\infty}} = exp\left(-\left(\frac{t}{t_r}\right)^{\beta}\right) \quad , \qquad (10)$$

where $v_h(t)$ is the hole volume measured at time t, v_h^0 is the hole volume at $t = 0$ (equal to the mean hole volume determined previously, Section 3.1), v_h^{∞} is the asymptotic hole volume value (equivalent to the equilibrium value), t_r is the relaxation time, and β is the exponent that characterizes the kinetic process. The KWW function has been widely used to describe the relaxation phenomena of the molecular mobility of polymers (Rabiei et al., 2016; Roggero et al., 2021). Generally, the heterogeneous dynamics of solid-state segmental regions lead to a distribution of relaxation times that are not well represented by a single exponential function. In this context, the exponent β of the KWW function characterizes the width of the spectrum of relaxation times. When $\beta = 1$, the function turns a single exponential decay function, while smaller values are related to wider distributions of relaxation times, which indicates that different processes occur.

The resulting parameters of fitting the experimental data with the KWW function are presented in Table 4. Particularly, the mean hole volume of TPS at equilibrium (RH=20%) turned out ~43 Å^3, showing a ~37% decrease to the initial value (RH=58%, Table 3). Volume at equilibrium was significantly lower in TPS-CA1 and TPS-CA5 to TPS, though there were no significant differences between the two TPS-CA films. Relaxation time was also significantly lower in TPS-CA1 and TPS-CA5 to TPS. A lower relaxation time indicates a faster decrease in the hole volume, which could be related to faster water desorption. The exponent β value was close to 1 for TPS films, showing that the kinetic of the hole volume during desorption is well-represented by a single exponential function. On the other hand, the exponent β was slightly slower in TPS-CA1 and TPS-CA5 to TPS, suggesting that different processes occur during hole volume evolution. The lower β values obtained for the TPS-CA films to TPS film can be correlated with the wider distributions of the hole volume in these materials (Section 3.1), as evidenced in the semi-widths at half height values (H_+, Table 3).

Table 4. Fitting parameters of mean hole volumes as a function of time (Fig. 2) using the KWW function. The values are reported as average ± standard error.

	v_h^0 (Å^3)	v_h^∞ (Å^3)	t_r(h)	β	R^2
TPS	67.6 ± 0.3^a	42.9 ± 0.4^a	33 ± 1^a	1.1 ± 0.1^a	0.989
TPS-CA1	66.0 ± 0.4^b	39 ± 2^b	20 ± 4^b	0.7 ± 0.2^b	0.888
TPS-CA5	65.7 ± 0.4^b	38.2 ± 0.9^b	22 ± 2^b	0.9 ± 0.1^b	0.951

Different letters within the same column indicate statistically significant differences ($p < 0.05$).

Figure 3 presents the mean hole volume (v_0) measured at equilibrium (RH=58%, Table 3), and the asymptotic value (v_∞, RH=20%) to the citric acid concentration. It is noticeable that both parameters decrease similarly when increasing citric acid concentration. The most notorious differences in the values were found between TPS and TPS-CA1 films, while there were no significant differences between TPS-CA1 and TPS-CA5 films. Moreover, the decrease of v_∞ was more pronounced that v_0 decrease, ranging from (42.9 ± 0.4) Å^3 to (38.2 ± 0.9) Å^3 in TPS and TPS-CA5 films, respectively. This result shows that the nano-structural changes are more significant for samples stabilized at low relative humidity, which could be availed for future studies on other thermoplastic starch-based films.

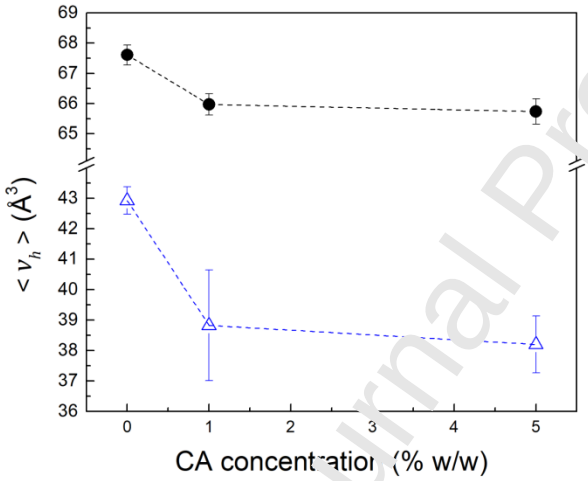

Figure 3. Mean hole volume at different relative humidity RH=58% (v_h^0: ●) and RH=20% (v_h^∞:Δ) as a function of CA concentration. Dashed lines are visual guides.

Figure 4 compares the hole volume distributions of the samples stabilized at RH=58% (reported previously in Fig. 1) with those corresponding to the samples stabilized at RH=20%. There was a systematic narrowing and shift to lower values of the hole volume distributions after water desorption and stabilization at lower relative humidity. In particular, the probability of hole volumes higher than 90 Å^3 is negligible in samples stabilized at RH=20%. According to these results, the loss of water molecules during desorption leads to a more closed structure, which corresponds to less plasticized materials.

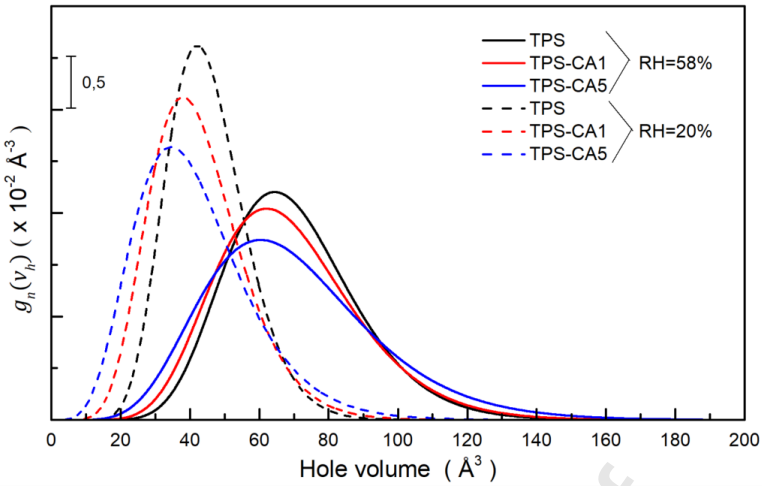

Figure 4. Hole volume probability distributions for the TPS-based films stabilized at RH=58% and RH=20%.

3.3 Influence of the hole volume distributions on water susceptibility and mechanical properties of the films

Table 5 presents water susceptibility parameters for the different materials. All films preserve their integrity after the assays and water solubility did not show significant differences between the developed materials ($p < 0.05$). The soluble fraction of the films could be related to the plasticizers (glycerol, sorbitol) that migrate to the water during immersion. On the other hand, MC depended on the CA concentration. TPS-CA1 presents a significantly lower MC value to TPS ($p < 0.05$). This difference could be a consequence of the lower mean free volume of nanoholes, as reported in Section 3.1. Additionally, the ester bonds formed between citric acid and starch could diminish the relative amount of hydroxyl groups, leading to lower affinity with ambient humidity (see FTIR section in Supplementary Material). However, TPS-CA5 shows a significantly higher value of MC to TPS and TPS-CA1. On the one hand, the higher CA concentration could lead to higher free CA molecules migrating to the surface which increases water uptake. On the other hand, the water absorption was favoured by a more open structure of the network of this material, which was revealed in the free hole volume distribution as an increase of the larger holes (Section 3.1). In previous research, it has been demonstrated by low-field nuclear magnetic resonance that CA crosslinking of TPS films leads to an open network, which occurs because CA reacts with both starch and plasticizers (Gonzalez-Seligra et al., 2016).

WVP did not show significant differences between TPS and TPS-CA1, but it was significantly higher in TPS-CA5. This result is consistent with the more open polymeric structure of this material. A similar effect was reported when incorporating 10% of CA in thermoplastic starch films obtained by casting method (González-Seligra et al., 2016).

The analysis of water susceptibility of TPS-CA5 in comparison with TPS and TPS-CA1 agrees with the PALS results. The films with higher water content (TPS-CA5) would be more plasticized precisely because of water. In the hole volume distribution, water plasticization would increase the number of larger holes (100-140 Å^3), which corresponds to a more open network in which water molecules diffusion results higher.

Table 5. Water solubility, moisture content and water vapour permeability of the different TPS-

based films. The values are reported as average ± standard error.

	WS (%)	MC (%)	WVP (g m^{-1} s^{-1} Pa^{-1} x 10^{-10})
TPS	24 ± 1[a]	20 ± 1[a]	3.5 ± 0.6[a]
TPS-CA1	26 ± 3[a]	15 ± 1[b]	2.9 ± 0.6[a]
TPS-CA5	22 ± 2[a]	29 ± 2[c]	8 ± 1[b]

Different letters within the same column indicate statistically significant differences ($p < 0.05$).

Free hole volume constitutes a nanostructural parameter of polymeric systems that can be correlated with several macroscopic properties; for example, the mechanical behaviour of thermoplastics varies with free hole volume (Blanco et al., 2009). In the present research, stress-strain tests were performed on TPS-based films immediately after removing the samples from the desiccator in which they were stabilized (RH=58%), and after 5 h of exposure to the laboratory atmosphere (RH=45%). Representative stress-strain curves are presented in Figure 5. Young's modulus significantly increased after exposure to the laboratory atmosphere. In particular, the increase was ~150%, ~50% and ~260% for TPS, TPS-CA1 and TPS-CA5 films, respectively. On the other hand, for the same exposure time, a decrease in the mean hole volume of ~4%, ~13%, and ~10% was observed for TPS, TPS-CA1, and TPS-CA5, respectively. Considering these results, it can be concluded that there exists a correlation between the relative changes in Young's modulus and mean hole volumes: a larger decrease of $\langle v_h \rangle$ corresponds to a larger increase in Young's modulus. It is worth mentioning that uniaxial tensile tests were performed at a strain rate in which the free hole volume is not expected to significantly change (each test takes less than 2 min).

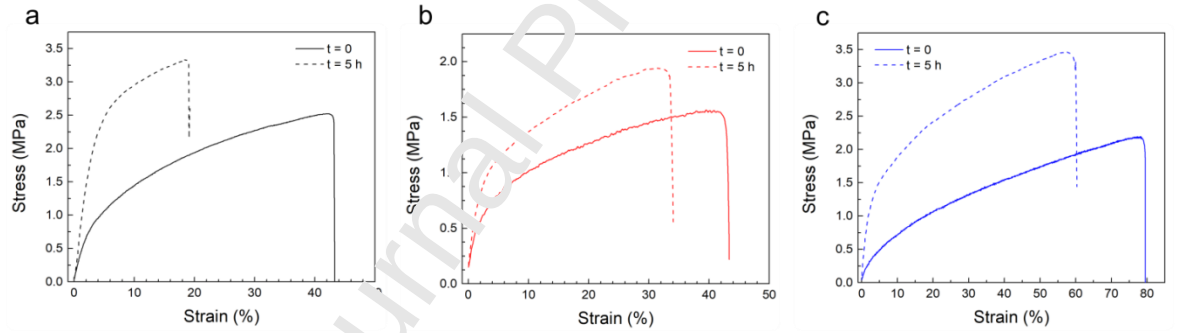

Fig. 5. Stress-strain curves obtained for the TPS (a), TPS-CA1 (b) and TPS-CA5 (c) films tested at controlled RH (58%) and after an exposure time in a dried atmosphere of 5 h.

Table 6. Young's modulus (E), stress at break (σ_b) and elongation at break (ε_b) of the TPS-based films stabilized at RH=58% ($t = 0$) and after exposure to labs atmosphere ($t = 5\ h$). The values are reported as average ± standard error.

	$E\ (MPa)$		$\sigma_b (MPa)$		$\varepsilon_b (\%)$	
	$t = 0\ h$	$t = 5\ h$	$t = 0\ h$	$t = 5\ h$	$t = 0\ h$	$t = 5\ h$
TPS	34 ± 3[a]	85 ± 5[a]	2.6 ± 0.2[a]	3.3 ± 0.1[a]	47 ± 4[a]	17 ± 1[a]
TPS-CA1	34 ± 2[a]	50 ± 4[b]	1.6 ± 0.3[b]	2.1 ± 0.1[b]	46 ± 3[a]	33 ± 5[b]
TPS-CA5	17 ± 1[b]	62 ± 2[c]	1.9 ± 0.3[b]	3.4 ± 0.1[a]	78 ± 10[b]	58 ± 7[c]

Different letters within the same column indicate statistically significant differences ($p < 0.05$).

The mechanical properties of TPS-based films have been measured by many authors. When comparing Young's modulus values reported in the literature differences up to one order of magnitude are found. The present research might contribute to understanding the origin of the significant dispersion in the experimental values. Starch characteristics (such as source, amylopectin/amylose ratio,

and molecular weight) are intrinsic to each system and can lead to variability in the properties of the TPS-based films. However, a difference between the relative humidity at which the samples are stored to the relative humidity in which they are tested could be critical because the nanostructure changes as the plasticizer content do. The difference between relative humidity at storage and testing leads to a humidity gradient which induces water molecules to migrate. Consequently, when performing mechanical properties tests on hygroscopic polymeric systems, it is necessary to know the relative humidity values during the storage of the samples and, also, throughout the mechanical tests.

4. Conclusions

This research demonstrates that the free volume properties of TPS films are susceptible to changes in moisture content and that the citric acid incorporation modifies the kinetics of the hole volume evolution during moisture conditioning. For stabilized samples, the distribution of hole volumes resulted slightly differently. The incorporation of 5% (w/w) citric acid leads to a wider distribution, which was associated with the higher moisture content of the samples. Likewise, it was demonstrated that the hole volume distributions narrow with the loss of moisture in all the studied materials. The biggest challenge to using TPS-based films for technological applications is to gain control of the structural variations of the material under different atmospheric conditions. Despite the effect of moisture on free volume properties having already been studied, the previous research has focused on carbohydrate polymer samples stabilized at different relative humidity. In the present paper, it was possible to study the evolution of free volumes in samples stored under non-equilibrium moisture conditions. An experimental arrangement in which the holes volumes are measured continuously and *in situ* during water desorption was proposed. From the obtained results, CA incorporation into TPS modifies the hole volume distributions and also the hole volume evolution kinetics during water desorption. The proposed experiment could be suitable for studying other kinetic processes in similar materials, such as the retrogradation of starch. Besides, it could be suitable to study the stability of materials against relative humidity.

Beyond the nanoscopic level, the results obtained in this paper are of utmost importance when dealing with practical applications, especially those where the measurement times are long (for example, creep testing). Summarizing, from a careful study of the nanostructural evolution of polymer hygroscopic systems it is possible to shed light on the understanding of unexpected results of micro and macroscopic experimental mechanical parameters.

Fundings

The authors would like to thank *Cooperativa Agrícola e Industrial San Alberto Limitada* (C.A.I.S.A., Misiones, Argentina). This work was supported by Agencia Nacional de Promoción Científica y Tecnológica (ANPCyT PICT 2017-2362, PICT 2015-1068, PICT 2015-1832), Secretaría de Políticas Universitarias (SPU No. 1655), Universidad de Buenos Aires (UBACyT 2018 20020170100381BA).

Declarations of interest: none.

References

Blanco, M., Ramos, J. A., Goyanes, S., Rubiolo, G., Salgueiro, W., Somoza, A., & Mondragon, I. (2009). Intermolecular interactions on amine-cured epoxy matrices with different crosslink densities. Influence on the hole and specific volumes and the mechanical behavior. *Journal of Polymer Science Part B: Polymer Physics*, *47*(13), 1240–1252.

https://doi.org/10.1002/polb.21729
Chalykh, A. E., Bardyshev, I. I., & Petrova, T. F. (2021). Free volume and water sorption by cellulose esters. *Polymers*, *13*(16), 2644. https://doi.org/10.3390/polym13162644
Cheng, N., Huang, Y., Dai, D., & Yeh, J. (2021). Oxygen barrier films of scCO2-assisted thermoplastic starch/poly (vinyl alcohol) blends. *Journal of Polymer Research*, *28*(12), 1–16. https://doi.org/10.1007/s10965-021-02824-3
Cunniff, P. A., & Jee, M. H. (1995). Official Methods of Analysis of AOAC International (16th edn). *Trends in Food Science and Technology*, *6*(11), 382.
Diyana, Z. N., Jumaidin, R., Selamat, M. Z., Ghazali, I., Julmohammad, N., Huda, N., & Ilyas, R. A. (2021). Physical properties of thermoplastic starch derived from natural resources and its blends: a review. *Polymers*, *13*(9), 1396. https://doi.org/10.3390/polym13091396
Dlubek, G., Fretwell, H. M., & Alam, M. A. (2000). Positron/positronium annihilation as a probe for the chemical environment of free volume holes in polymers. *Macromolecules*, *33*(1), 187–192. https://doi.org/10.1021/ma9904215
Dlubek, G., Sen Gupta, A., Pionteck, J., Krause-Rehberg, R., Kaspar, H., & Lochhaas, K. H. (2004). Temperature dependence of the free volume in fluoroelastomers from positron lifetime and PVT experiments. *Macromolecules*, *37*(17), 6606–6618.
Eldrup, M., Lightbody, D., & Sherwood, J. N. (1981). The temperature dependence of positron lifetimes in solid pivalic acid. *Chemical Physics*, *63*(1–2), 51–58. https://doi.org/10.1016/0301-0104(81)80307-2
Estevez-Areco, S., Guz, L., Candal, R., & Goyanes, S. (2020). Active bilayer films based on cassava starch incorporating ZnO nanorods and PVA electrospun mats containing rosemary extract. *Food Hydrocolloids*, *108*, 106054. https://doi.org/10.1016/j.foodhyd.2020.106054
Estevez-Areco, S., Guz, L., Famá, L., Candal, R., & Goyanes, S. (2019). Bioactive starch nanocomposite films with antioxidant activity and enhanced mechanical properties obtained by extrusion followed by thermo-compression. *Food Hydrocolloids*. https://doi.org/10.1016/j.foodhyd.2019.05.054
Famá, L., Goyanes, S., & Gerschenson, L. (2007). Influence of storage time at room temperature on the physicochemical properties of cassava starch films. *Carbohydrate Polymers*, *70*(3), 265–273. https://doi.org/10.1016/j.carbpol.2007.04.003
Famá, L., Rojo, P. G., Bernal, C., & Goyanes, S. (2012). Biodegradable starch based nanocomposites with low water vapor permeability and high storage modulus. *Carbohydrate Polymers*, *87*(3), 1989–1993.
Florez, J. P., Fazeli, M., & Simão, R. A. (2019). Preparation and characterization of thermoplastic starch composite reinforced by plasma-treated poly (hydroxybutyrate) PHB. *International Journal of Biological Macromolecules*, *123*, 609–621. https://doi.org/10.1016/j.ijbiomac.2018.11.070
Geyer, R. (2020). Production, use, and fate of synthetic polymers. In *Plastic waste and recycling* (pp. 13–32). Elsevier. https://doi.org/10.1016/B978-0-12-817880-5.00002-5
Giacinti Baschetti, M., & De Angelis, M. G. (2015). 8 - Vapour permeation modelling. In A. Basile, A. Figoli, & M. B. T.-P. Khayet Vapour Permeation and Membrane Distillation (Eds.), *Pervaaporation, Vapour Permeation and Membrane Distillation* (pp. 203–246). Woodhead Publishing. https://doi.org/10.1016/B978-1-78242-246-4.00008-8
Giebel, D., & Kansy, J. (2011). A new version of LT program for positron lifetime spectra analysis. *Materials Science Forum*, *666*, 138–141.

https://doi.org/10.4028/www.scientific.net/MSF.666.138

González-Seligra, P., Guz, L., Ochoa-Yepes, O., Goyanes, S., & Famá, L. (2017). Influence of extrusion process conditions on starch film morphology. *Lwt*, *84*, 520–528. https://doi.org/10.1016/j.lwt.2017.06.027

Gonzalez-Seligra, P., Jaramillo, C. M., Famá, L., & Goyanes, S. (2016). Biodegradable and non-retrogradable eco-films based on starch–glycerol with citric acid as crosslinking agent. *Carbohydrate Polymers*, *138*, 66–74. https://doi.org/10.1016/j.carbpol.2015.11.041

Guarás, M. P., Ludueña, L. N., & Alvarez, V. A. (2020). Recent advances in thermoplastic starch biodegradable nanocomposites. *Handbook of Nanomaterials and Nanocomposites for Energy and Environmental Applications*, 1–24.

Guz, L., González-Seligra, P., Ochoa-Yepes, O., Estevez-Areco, S., Famá, L., & Goyanes, S. (2020). Influence of Different Commercial Modified Cassava Starches on the Physicochemical Properties of Thermoplastic Edible Films Obtained by Flat-die Extrusion. *Starch - Stärke*, 2000167. https://doi.org/10.1002/star.202000167

Hughes, D., Tedeschi, C., Leuenberger, B., Roussenova, M., Coveney, A., Richardson, R., Bönisch, G. B., Alam, M. A., & Ubbink, J. (2016). Amorphous-amorphous phase separation in hydrophobically-modified starch–sucrose blends II. Crystallinity and local free volume investigation using wide-angle X-ray scattering and positron annihilation lifetime spectroscopy. *Food Hydrocolloids*, *58*, 216–223. https://doi.org/10.1016/j.foodhyd.2016.01.024

Jean, Y. C. (1990). Positron annihilation spectroscopy for chemical analysis: a novel probe for microstructural analysis of polymers. *Microchemical Journal*, *42*(1), 72–102. https://doi.org/10.1016/0026-265X(90)90027-3

Jean, Y. C., Mallon, P. E., & Schrader, D. M. (2003). Principles and Application of Positron and Positronium Chemistry, World Sci. *Publ. Co. Pte. Ltd., New Jersy-London-Singapore-Hong Kong*.

Kilburn, D., Claude, J., Mezzenga, R., Dlubek, G., Alam, A., & Ubbink, J. (2004). Water in glassy carbohydrates: opening it up at the nanolevel. *The Journal of Physical Chemistry B*, *108*(33), 12436–12441. https://doi.org/10.1021/jp048774f

Kilburn, D., Claude, J., Schweizer, T., Alam, A., & Ubbink, J. (2005). Carbohydrate polymers in amorphous states: An integrated thermodynamic and nanostructural investigation. *Biomacromolecules*, *6*(2), 864–879. https://doi.org/10.1021/bm049355r

Kobayashi, Y., Zheng, W., Meyer, E. F., McGervey, J. D., Jamieson, A. M., & Simha, R. (1989). Free volume and physical aging of poly (vinyl acetate) studied by positron annihilation. *Macromolecules*, *22*(5), 2302–2306.

Langer, E., Bortel, K., Waskiewicz, S., & Lenartowicz-Klik, M. (2020). 1 - Assessment of Traditional Plasticizers. In E. Langer, K. Bortel, S. Waskiewicz, & M. B. T.-P. D. from P.-C. P. E. T. Lenartowicz-Klik (Eds.), *Plasticizers Derived from Post-Consumer PET* (pp. 1–11). William Andrew Publishing. https://doi.org/10.1016/B978-0-323-46200-6.00001-5

Lin, B., Du, Y., Li, Y., Liang, X., Wang, X., Deng, W., Wang, X., Li, L., & Kennedy, J. F. (2010). The effect of moist heat treatment on the characteristic of starch-based composite materials coating with chitosan. *Carbohydrate Polymers*, *81*(3), 554–559. https://doi.org/10.1016/j.carbpol.2010.03.006

Maizura, M., Fazilah, A., Norziah, M. H., & Karim, A. A. (2007). Antibacterial activity and mechanical properties of partially hydrolyzed sago starch–alginate edible film containing lemongrass oil. *Journal of Food Science*, *72*(6), C324–C330.

Martini, F., Hughes, D. J., Bönisch, G. B., Zwick, T., Schäfer, C., Geppi, M., Alam, M. A., & Ubbink, J. (2020). Antiplasticization and phase behavior in phase-separated modified starch-sucrose blends: A positron lifetime and solid-state NMR study. *Carbohydrate Polymers*, *250*, 116931. https://doi.org/10.1016/j.carbpol.2020.116931

Medina Jaramillo, C., Gonzalez Seligra, P., Goyanes, S., Bernal, C., & Famá, L. (2015). Biofilms based on cassava starch containing extract of yerba mate as antioxidant and plasticizer. *Starch-Stärke*, *67*(9–10), 780–789. https://doi.org/10.1002/star.201500033

Rabiei, N., Kish, M. H., & Amirshahi, S. H. (2016). Monitoring the structural relaxation in poly (ethylene terephthalate) fibers: Dye sorption and FTIR considerations. *Polymer*, *106*, 72–84. https://doi.org/10.1016/j.polymer.2016.10.048

Reddy, N., & Yang, Y. (2010). Citric acid cross-linking of starch films. *Food Chemistry*, *118*(3), 702–711. https://doi.org/10.1016/j.foodchem.2009.05.050

Ribba, L., Garcia, N. L., D'Accorso, N., & Goyanes, S. (2017). Disadvantages of starch-based materials, feasible alternatives in order to overcome these limitations. In *Starch-based materials in food packaging* (pp. 37–76). Elsevier.

Roggero, A., Caussé, N., Dantras, E., Villareal, L., Santos, A., & Pébère, N. (2021). In situ study of the temperature activated kinetics of water sorption in an epoxy varnish. *Polymer*, *213*, 123206. https://doi.org/10.1016/j.polymer.2020.123206

Rosenboom, J.-G., Langer, R., & Traverso, G. (2022). Bioplastics for a circular economy. *Nature Reviews Materials*, *7*(2), 117–137. https://doi.org/10.1038/s41578-021-00407-8

Roussenova, M., Murith, M., Alam, A., & Ubbink, J. (2010). Plasticization, antiplasticization, and molecular packing in amorphous carbohydrate-glycerol matrices. *Biomacromolecules*, *11*(12), 3237–3247. https://doi.org/10.1021/bm1005068

Salihu, R., Abd Razak, S. I., Zawawi, N. A., Kadir, M. R. A., Ismail, N. I., Jusoh, N., Mohamad, M. R., & Nayan, N. H. M. (2021). Citric acid: A green cross-linker of biomaterials for biomedical applications. *European Polymer Journal*, *146*, 110271. https://doi.org/10.1016/j.eurpolymj.2021.110271

Shakespeare, W. (2002). CHAPTER 3 - THE GLASS TRANSITION PHENOMENON. In K. J. B. T.-S. C. of G. Rao (Ed.), *Structural Chemistry of Glasses* (pp. 77–135). Elsevier Science Ltd. https://doi.org/10.1016/B978-008043958-7/50021-2

Shi, R., Zhang, Z., Liu, Q., Han, Y., Zhang, L., Chen, D., & Tian, W. (2007). Characterization of citric acid/glycerol co-plasticized thermoplastic starch prepared by melt blending. *Carbohydrate Polymers*, *69*(4), 748–755. https://doi.org/10.1016/j.carbpol.2007.02.010

Standard, A. (2004). D882-02. *ASTM Standard Test Method for Tensile Properties of Thin Plastic Sheeting*.

Wang, X., Huang, L., Zhang, C., Deng, Y., Xie, P., Liu, L., & Cheng, J. (2020). Research advances in chemical modifications of starch for hydrophobicity and its applications: A review. *Carbohydrate Polymers*, *240*, 116292. https://doi.org/10.1016/j.carbpol.2020.116292

Zhang, Y., Rempel, C., & Liu, Q. (2014). Thermoplastic starch processing and characteristics—a review. *Critical Reviews in Food Science and Nutrition*, *54*(10), 1353–1370. https://doi.org/10.1080/10408398.2011.636156

Authorship contribution statement

Santiago Estevez-Areco: Methodology, Investigation, Formal analysis, Visualization, Writting - Original Draft; Carlos Macchi: Methodology, Investigation, Formal analysis, Visualization, Writting - Review & Editing; Lucas Guz: Methodology, Investigation, Formal analysis, Writting - Review & Editing; Silvia Goyanes: Supervision, Project Administration, Funding acquisition, Writting - Review & Editing; Alberto Somoza: Supervision, Project Administration, Funding acquisition, Writting - Review & Editing.

Declaration of interests

☒ The authors declare that they have no known competing financial interests or personal relationships that could have appeared to influence the work reported in this paper.

☐The authors declare the following financial interests/personal relationships which may be considered as potential competing interests:

Graphical abstract